PLASMONIC SENSOR FOR DETECTION OF β-LACTAM ANTIBIOTICS BASED ON THE CONJUGATED ANTIBODY WITH GOLD NANOPARTICLES **

M. Aghamirzaei [1], M. S. Khiabani [1*], H. Hamishehkar [2], R. R. Mokarram [1], M. Amjadi [1]

[1] University of Tabriz, Tabriz, Iran; e-mail: m.sowti@tabrizu.ac.ir, sowti_m@yahoo.com
[2] Drug Applied Research Center at Tabriz University of Medical Sciences, Tabriz, Iran

This study aims to detect β-lactam antibiotics using a conjugated antibody with gold nanoparticles (GNPs). For this purpose, the gold nanoparticles synthesized from Chinese lettuce leaf extract (as reductant) were used for the colorimetric detection of β-lactam antibiotics (such as ampicillin, amoxicillin, penicillin G, oxacillin, and carbenicillin). XRD, FTIR spectroscopy, TEM, and dynamic light scattering were utilized to detect the crystallinity, to identify functional groups involved in the synthesis of GNPs, and to measure the size of the GNPs; pH 8 and a concentration of 8.4 μg of antibody at 1 mL GNPs solution were selected as the best pH and concentration of antibody for the conjugation of antibody with GNPs. The maximum wavelengths of the colloidal GNPs, conjugation of antibody with GNPs, and detection of antibiotics (from 1 nM to 1 mM) with GNPs-PAb were recorded using a micro-volume spectrophotometer system. The results indicated that the localized surface plasmon resonance spectrometer absorption wavelength of GNPs red-shifted with increasing concentration of β-lactam antibiotics. With increasing concentration of ampicillin, penicillin G, and carbenicillin, the wavelength of maximum changed, and after saturation of antibiotics concentration, the curve reaches a plateau. This indicated that the antibody showed similar behavior in the detection of these antibiotics. But regarding amoxicillin, the saturation concentration is much higher, indicating that the antibody was more specific for its detection. In contrast, for oxacillin, saturation occurred very soon, which demonstrated that the antibody had an extremely low detection capability for this antibiotic. Finally, the results showed that the antibody was sensitive to 1 nM of the five β-lactam antibiotics studied.

Keywords: *localized surface plasmon resonance spectrometer, β-lactam antibiotics, polyclonal antibody of β-lactam, gold nanoparticles, conjugation.*

ПЛАЗМОННЫЙ СЕНСОР ДЛЯ ОБНАРУЖЕНИЯ β-ЛАКТАМНЫХ АНТИБИОТИКОВ НА ОСНОВЕ КОНЪЮГИРОВАННОГО АНТИТЕЛА С НАНОЧАСТИЦАМИ ЗОЛОТА

M. Aghamirzaei [1], M. S. Khiabani [1*], H. Hamishehkar [2], R. R. Mokarram [1], M. Amjadi [1]

УДК 535.853.4;620.3

[1] Университет Тебриза, Тебриз, Иран; e-mail: m.sowti@tabrizu.ac.ir, sowti_m@yahoo.com
[2] Центр прикладных исследований медикаментов Тебризского медицинского университета, Тебриз, Иран

(Поступила 10 декабря 2019)

Предложен сенсор для обнаружения β-лактамных антибиотиков, основанный на использовании антител, связанных с наночастицами золота (НЧ-Аи). Для колориметрического определения β-лактамных антибиотиков (ампициллина, амоксициллина, пенициллина G, оксациллина и карбенициллина) в качестве восстановителя задействованы НЧ-Аи, синтезированные из экстракта листьев китайского салата. Методы рентгеновской дифракции, ИК-Фурье-спектроскопии, просвечивающей электронной микроскопии и динамического рассеяния света использованы для обнаружения кристалличности, идентификации функциональных групп, участвующих в синтезе НЧ-Аи, и измерения

** Full text is published in JAS V. 88, No. 1 (http://springer.com/journal/10812) and in electronic version of ZhPS V. 88, No. 1 (http://www.elibrary.ru/title_about.asp?id=7318; sales@elibrary.ru).

их размера. В качестве наилучших значений выбраны pH 8, концентрация антител в 1 мл раствора НЧ-Аи 8.4 мкг. С помощью спектрофотометра зарегистрированы спектры коллоидных НЧ-Аи, антител, связанных с НЧ-Аи, и антибиотиков (с концентрацией от 1 нМ до 1 мМ) в присутствии системы антитела–НЧ-Аи. Показано, что с увеличением концентрации β-лактамных антибиотиков линия поглощения НЧ-Аи сдвигается в красную область. При увеличении концентрации ампициллина, пенициллина G и карбенициллина длина волны максимума изменяется, однако по достижении некоторой концентрации антибиотиков (уровня насыщения) кривая выходит на плато, что указывает на влияние антител при обнаружении этих антибиотиков. Для амоксициллина концентрация насыщения намного выше, что указывает на особую роль антител при его обнаружении. Для оксациллина насыщение наступает очень быстро. Это демонстрирует, что антитела обладают чрезвычайно низкой способностью обнаружения данного антибиотика. Наличие антител позволяет обнаружить пять β-лактамных антибиотиков с чувствительностью до 1 нМ.

Ключевые слова: *спектрометр локализованного поверхностного плазмонного резонанса, β-лактамные антибиотики, поликлональные антитела к β-лактаму, наночастицы золота, конъюгация.*

Introduction. Antibiotics of the β-lactam group are part of a wide variety of antimicrobial agents used for the treatment of bacterial infections of animals in livestock farming. β-Lactams consist of four groups: penicillins, cephalosporins, carbapenems, and monobactams. Residual β-Lactams in food can seriously cause allergic reactions and develop resistant strains in consumers. Also, they can cause serious economic problems for producers of milk and dairy products. For example, they decrease the acid and flavor of butter and reduce the curdling of the milk and cause unsuitable ripening of cheese.

Antibiotics are detected using an instrumental technique such as high-performance liquid chromatography/mass spectrometry (HPLC/MS) [1] and gas chromatography/mass spectrometry (GC/MS) [2], and sensors based on the antibody-antigen interaction, such as enzyme-linked immunosorbent assay (ELISA) [3], fluorescence polarization immunoassay [4], immunosensor assay [5], and UV and localized surface plasmon resonance (LSPR) [6, 7].

In recent years, gold nanoparticles (GNPs) have been used to detect pharmaceutical samples due to their excellent properties such as unique optical and electronic properties, biocompatibility, stability, and high extinction coefficients [7, 8–18]. GNPs can be conjugated with the antibody and used to detect antibiotics based on the colorimetric method (absorbance intensity change or change the LSPR wavelength) [19]. The LSPR band is produced in GNPs due to collective oscillations of free electrons. Free electrons have a natural frequency of oscillation .When this frequency matches the frequency of incident radiation, a major LSPR band is produced with the absorption of light. There is a direct correlation between sensitivity of antibodies and change in intensity of absorption and the wavelength of a maximum. If the antibody has high sensitivity, as the concentration of antibiotics increases, the absorption intensity and the LSPR wavelength change significantly. But if the antibody has low sensitivity, the intensity wavelength does not change much. However, to use this method, the antibody must be properly conjugated with the GNPs. Therefore, several factors such as the amount of antibody and pH were evaluated for proper conjugation [20]. The purpose of this study is to use antibody conjugated with the GNPs to detect β-lactam antibiotics by the LSPR technique.

Materials. Sheep polyclonal β-lactam antibody (PAb) was purchased from MyBioSource Co. (California, USA). Chloroauric acid ($HAuCl_4 \cdot 3H_2O$) was obtained from Jieding Tech Co. (Shanghai, China). The ampicillin sodium salt, penicillin G potassium salt, amoxicillin, oxacillin sodium salt monohydrate, and carbenicillin disodium salt were purchased from Sigma-Aldrich (St. Louis, USA). pH indicator paper and potassium carbonate were obtained from Merck (Darmstadt, Germany). Phosphate-buffered saline (PBS) powder was purchased from Biosera (France). The other chemicals used were of analytical grade. Distilled water used was purified using an ultra-pure water system from Millipore Co. (Bedford, MA, USA).

Methods. Colloidal GNPs were prepared from an aqueous extract of Chinese lettuce leaves as a reducing agent. Briefly, 3 mL of Chinese lettuce leaves extract were added to 2 mM solution of $AuCl_4 \cdot 3H_2O$ (pH 6) rapidly under constant stirring (100 rpm). The solution was kept at 70°C for 15 min until its color changed to a brilliant wine-red. Then the solution was cooled at room temperature and the prepared colloidal gold was stored at 4°C in the darkness for future use [21].

The average size and charge of the colloidal GNPs were measured by dynamic light scattering (DLS) using a particle size/zeta potential analyzer (Zetasizer Nano ZS, Malvern Instruments Ltd., UK).

To detect the morphology of the GNPs, transmission electron microscopy (TEM) (Jeol, Tokyo, Japan, at an accelerating voltage of 80,000 V and a magnification of 3,300,000) was used. GNPs was ultrasonicated

for 20 min and then coated on the ultraclean carbon copper grid for analysis [16].

FTIR analysis was carried out for the identification of functional groups involved in the synthesis of GNPs prepared from Chinese lettuce leaves extract. The freeze-dried samples of Chinese lettuce extract and GNPs were ground separately with KBR (FTIR grade) and analyzed by FTIR Nicolet Avatar 660 (Nicolet, USA) using transmittance mode at 4 cm^{-1} resolution. Then the spectra were recorded from 400–4000 cm^{-1} [22, 23].

To detect the crystallinity and the lattice properties of the GNPs, X-ray diffraction (XRD) (P Analytical, Philips PW 1830, The Netherlands) operating at 40 kV and 40 mA was applied. It is necessary to mention that the colloidal suspension containing GNPs was dried for 24 h by a freeze dryer [24].

To determine the effect of pH on the conjugation of PAb with GNPs, 500 µL of the colloidal gold solution was put into an Eppendorf tube, and pH of the colloidal gold from 6 to 12 was adjusted by K_2CO_3. Next, 10 µg/mL of PAb was added into each tube. Then, the mixtures were gently stirred and allowed to react for 15 min at room temperature. Subsequently, 50 µL of 10% NaCl solution was added to each tube. Finally, the absorbance of each mixture was determined at 525 nm using a micro-volume spectrophotometer [25].

To determine the effect of PAb concentration on the conjugation of PAb with GNPs, different concentrations of PAb (0, 0.5, 1, 1.5, 2, 2.5, 3, 3.5, 4, 4.5, and 5 µg/mL) were added to 500 µL of the colloidal gold solution with pH 8. Next, the resulting mixtures were gently stirred and allowed to react for 20 min at room temperature. Finally, 50 µL of NaCl solution (10%) was added to each of the tubes, and the absorbance of each mixture was measured at 525 nm [19].

For the evaluation of antibody conjugation with GNPs, the wavelength of a maximum and intensity of absorption of GNPs and conjugated GNPs with antibodies was measured by LSPR. The best conjugation occurs when there is little difference between the wavelength of a maximum of GNPs and the wavelength of a maximum of conjugated antibody-GNPs. The large difference between the wavelength of a maximum of GNPs and the wavelength of a maximum of conjugated antibody-GNPs is indicative of the accumulation of nanoparticles [20, 21].

To evaluate the detection accuracy of β-lactam antibiotics based on conjugated PAb with GNPs, different concentrations of βl antibiotics (ampicillin, amoxicillin, penicillin G, oxacillin, and carbenicillin) from 1 nM to 1 mM were utilized. The detection criterion in this method is based on changes in the absorption intensity and the wavelength using a micro-volume spectrophotometer (Nano Mabna Iranian Co., Iran) at the wavelength range of 400–800 nm [26].

Results and discussion. *DLS analysis.* From the dynamic light scattering results, the estimated average particle size distribution of GNPs and average zeta potential value were 50.4 nm and –7.89 mV, respectively (Figs. 1 and 2). The results of this study were consistent with the results of DLS analysis of the generated GNPs from leaf extract of *Ziziphus zizyphus* showed an average hydrodynamic diameter of 51.8 nm [27].

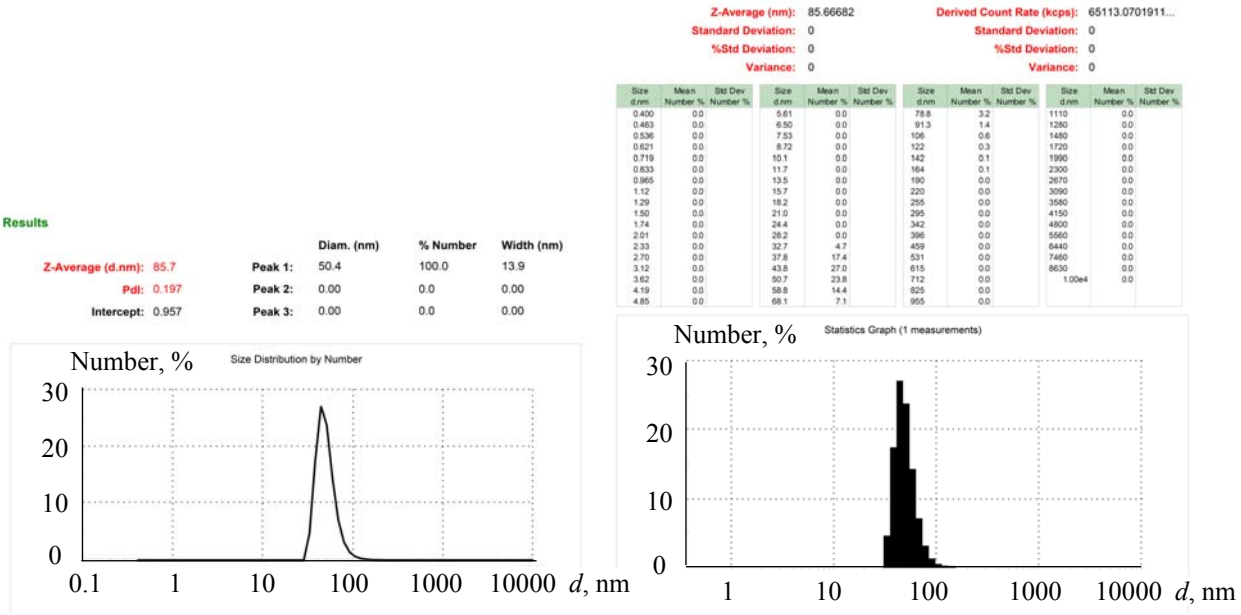

Fig. 1. Dynamic light scattering of GNPs.

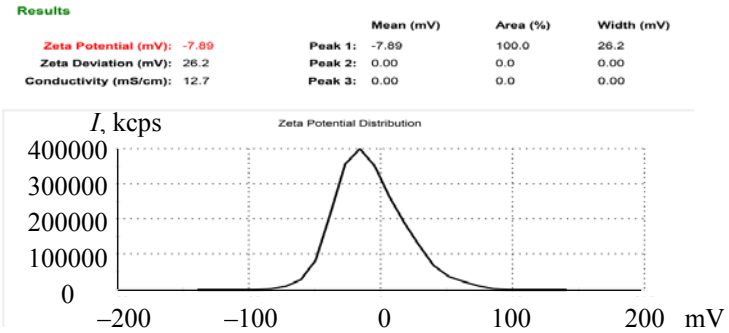

Fig. 2. Zeta potential of GNPs.

The zeta potential (electrokinetic potential) determines the nature and the extent of the interaction between particles and liquid medium. It is an important index of the colloidal stability of liquid dispersions. This parameter may be positive or negative, but values greater than –30 mV or +30 mV led to the good quality and stability of nanoparticles, which can be stored for a longer period. Given that the zeta potential of GNPs was negative (–7.89 mV), they were stable at refrigerator temperature for 6 months, and no precipitates and aggregates were observed in the colloid solution. The reason can be attributed to the capping of protein biomass constituents present in the extract [28].

TEM. Figure 3 shows the images of the TEM of synthesized GNPs. The images show that the resulting nanoparticles are almost spherical with a mean size of almost 25 nm. However, the significant differences in the size of the nanoparticles by the two techniques of DLS (50.4 nm) (Fig. 1) and TEM can be related to the adsorption of macromolecules and strongly hydrophilic compounds on the surface of the nanoparticles (in DLS technique), resulting in high water sweating at the nanoparticles level; this caused the radius of hydrodynamics to increase [29].

XRD. Pattern of nanoparticles (Fig. 4) showed that GNPs at 38.79, 44.59, 65.05, and 78.09 have sharp peaks, which is a factor in the synthesis of GNPs. Structural analysis shows that nanoparticles have a crystalline structure with Miller indexes (1 1 1), (2 0 0), (2 2 0), and (3 1 1) in the cubic network. Similar results were reported for GNPs in the literature [30, 31]. By comparing the intensity of the peaks, it is clear that the peak (1 1 1) is more intense than other peaks, as a result of which crystalline nanoparticles are further formed in this direction. The reported peak values are also similar to the planes and face-centered cubic structures of GNPs produced by other green synthesis processes [32]. Usually, the broadening of peaks in the XRD patterns of solids is associated with particle size [33]. The XRD patterns, which match with the database of JCPDS file No. 04-0784, show that all types of synthesized GNPs from Chinese lettuce leave extract were of pure crystalline nature. Broader peaks signify smaller particle size and show the effects of test conditions (such as pH, temperature, the concentration of $AuCl_4 \cdot 3H_2O$, etc.) on the nucleation and growth of the crystal nuclei. The value of β is calculated using the Pert-X software and is equal to 0.0064 rad. By placing the corresponding parameters about $D = 0.9\lambda/\beta\cos\theta$, the crystal size was determined 23 nm. It is suggested that the (1 1 1) plane is the predominant orientation, as confirmed by the results of TEM (Fig. 3).

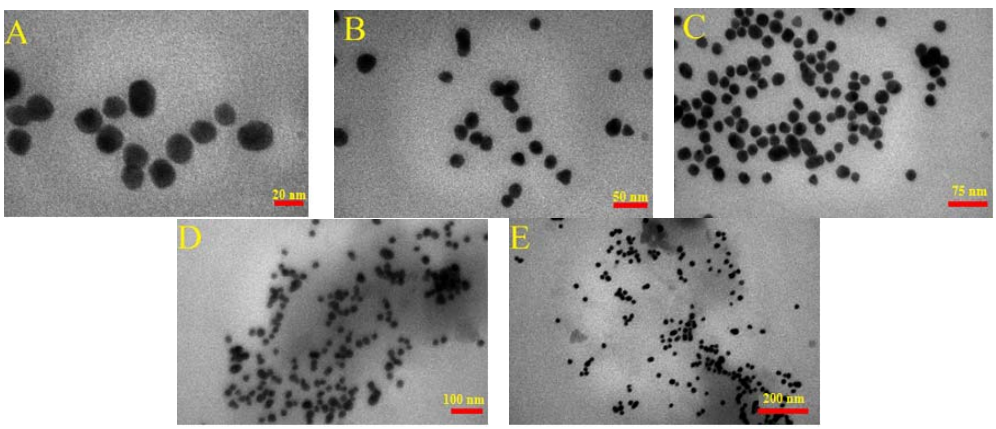

Fig. 3. TEM images of GNPs.

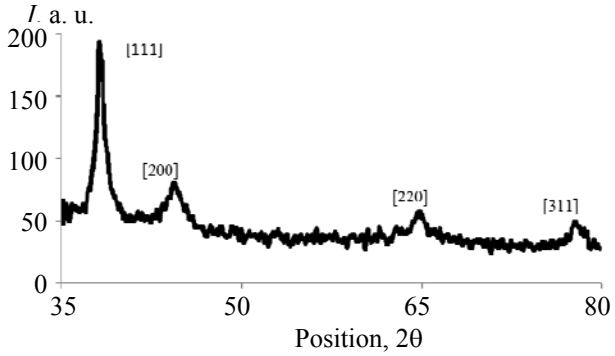

Fig. 4. X-ray diffraction spectrum of GNPs formed with the extracts of Chinese lettuce leaves.

FTIR spectra of Chinese lettuce leaf extract and the synthesized GNPs are shown in Fig. 5. Both spectra indicate the main characteristic peaks of Chinese lettuce leaf extract at 664, 671, and 703 cm^{-1} (C-Cl stretch, alkyl halide), 900 and 954 cm^{-1} (C=C stretch, alkene), 1029 and 1313 cm^{-1} (C-O stretch, ether), 1408 and 1437 cm^{-1} (CH2 stretch, alkane), 1659 cm^{-1} (C=C stretch, alkene), 2076 and 2105cm^{-1} (C≡C stretch, alkyne), 2913 and 2997 cm^{-1} (C-H sp3 stretch, alkane), and 3430 and 3432 cm^{-1} (O-H stretch, phenols). As explained in the Zeta potential section, the colloidal solutions of the GNPs were stable for 6 months at refrigerator temperature. Results of researches showed that the phytochemical constituents, especially alkane, alkene, ether, and phenols groups available in the extract, protect against aggregation and thereby retain the long-term stability of GNPs [34]. The difference in peak intensities of GNPs and extracts is nearly identical to the results of Gopinath et al. [35].

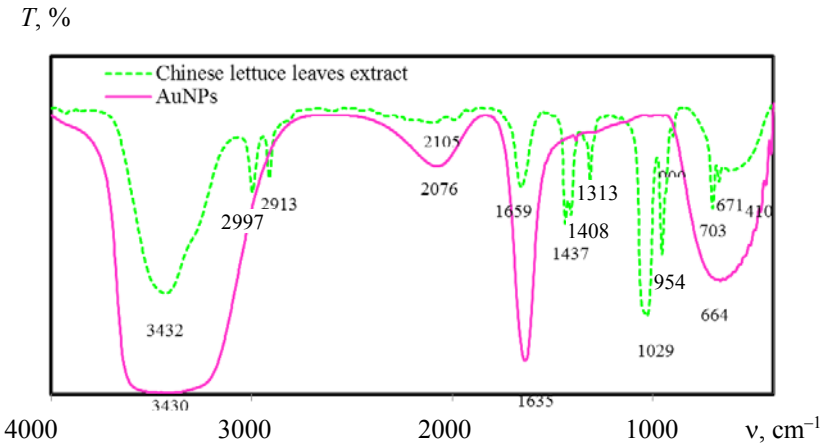

Fig. 5. FTIR spectrum of pure leaf extract of Chinese lettuce and reduced GNPs.

Effect of pH and PAb concentration on the conjugation of PAb with GNPs. The absorbance measurement results of GNPs-PAb conjugates solutions at different pH values at pH, 6, 7, 8, 9, 10, 11, and 12 OD_{525} = 0.665±0.035, 0.701±0.018, 0.754±0.008, 0.752±0.015, 0.753±0.021, 0.755±0.016, and 0.754±0.013, respectively. The data are expressed as mean ± standard deviation (SD) of three independent experiments. Different letters in columns show significant (p<0.05) differences between means.

For this purpose, seven series of solutions were made at different pH (6, 7, 8, 9, 10, 11, and 12) at room temperature, and the absorbance of solutions was measured by a spectrophotometer at 525 nm. The results indicated that by increasing pH, the OD_{525} rose. The highest amount of OD_{525} was observed at pH 8. No significant difference in OD_{525} was observed between pH 8 and pH higher than 8. Therefore, a pH of 8 was selected as the best pH for the conjugation of antibody with GNPs. The pH of the medium should be just above the isoelectric point of the antibody for suitable conjugation [13]. In a pH of less than antibody isoelectric pH, there is a negative charge for the protein, and conjugation does not completely occur due to the negative charge of the nanoparticles and the repulsion between the nanoparticles and the antibodies. Nevertheless, at pHs higher than isoelectric pH, GNPs form a stable hydrophobic solution because of electrostatic interaction and van der Waals force that is negatively charged, called colloidal gold [32, 36].

Thus, the positively charged antibodies and negatively charged colloidal gold solution conjugate firmly.

In the next stage, the effect of different concentrations of PAb (0.5, 1, 1.5, 2, 2.5, 3, 3.5, 4, 4.5, and 5) in the conjugation of PAb with GNPs was studied. Table 1 displays OD_{525} of GNPs conjugated at different concentrations of GNPs in pH 8. The results indicated that with increasing PAb concentration, OD_{525} decreased. The least amount of OD_{525} was observed in 3.5 µg of PAb. No significant difference in OD_{525} was observed between 3.5 µg PAb/500 µL and higher than 3.5 µg PAb/500 µL (Table 1). Therefore, 3.5 µg PAb/500 µL was selected as the best concentrations of PAb for the conjugation of antibody with GNPs. The results of previous studies indicated that the optimal amount for a practical application can be adjusted to 120% of the PAb concentration minimum [25]. Therefore, a concentration of 4.2 µg of antibody at 500 µL GNPs solution (i.e., 8.4 µg antibodies for 1 mL GNPs) is the best concentration for conjugation between the GNPs and the antibody.

TABLE 1. Effect of PAb Concentration on Conjugation of PAb with GNPs

PAb concentration, µg	OD_{525}
0	0.749 ± 0.014^{a}
0.5	0.724 ± 0.003^{b}
1	0.718 ± 0.006^{bc}
1.5	0.709 ± 0.007^{bcd}
2	0.705 ± 0.016^{cde}
2.5	0.701 ± 0.005^{cde}
3	0.7 ± 0.009^{de}
3.5	0.69 ± 0.001^{de}
4	0.691 ± 0.003^{de}
4.5	0.692 ± 0.013^{de}
5	0.689 ± 0.016^{e}

N o t e. The data are expressed as mean ±SD of three independent experiments. Different letters (a, b, c, d, and e) in columns show significant ($p < 0.05$) differences between means.

Evaluation of antibody conjugation with GNPs by LSPR. When the best pH and antibody concentration for conjugation with GNPs were obtained, conjugation of PAb with GNPs was investigated. As described before, the best conjugation occurs when there is a little difference between the maximum wavelength of GNPs and that of conjugated antibody-GNPs. A large difference between the wavelengths is indicative of the accumulation of nanoparticles [30]. Therefore, as can be seen from Fig. 6, it can be concluded that the conjugation is well completed due to the small difference between the wavelength of a maximum of the antibody (525 nm) and the wavelength of a maximum of conjugated antibody-GNPs (538 nm).

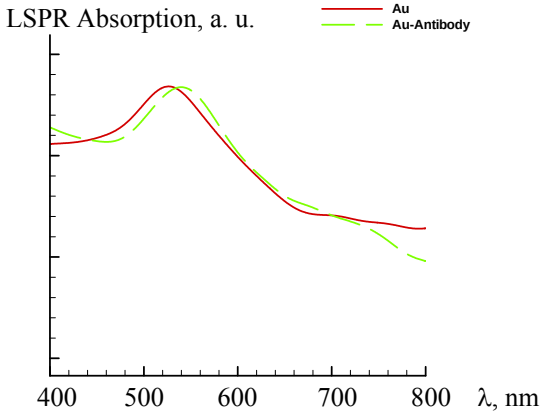

Fig. 6. The spectra of colloid gold (red line) and antibody-colloid gold conjugate (green line).

Evaluation of the PAb-GNP sensor for the detection of β-lactam antibiotics. PAb-GNPs were used for the detection of five β-lactam antibiotics (ampicillin, penicillin G, amoxicillin, carbenicillin, and oxacillin). If the antibody had high sensitivity, as the concentration of antibiotics increases, the intensity of absorption and the maximum wavelength exhibit more changes. However, if the antibody has low sensitivity, the intensity and wavelength do not change much. Figure 7 shows the LSPR absorption spectra of the GNPs-PAb solutions containing different concentrations of β-lactam antibiotics (ampicillin, penicillin G, amoxicillin, carbenicillin, and oxacillin). The results indicated that when concentrations of 0.01 μM of ampicillin, 0.1 μM of penicillin G, 1 μM of amoxicillin, 0.1 μM of carbenicillin, and 0.01 nM of oxacillin were used, the wavelength of a maximum (λ_{LSPR}) changed from 527 to 537, 531 to 539, 531 to 545, 532 to 540, and from 535 to 540 nm, respectively. This shows that the antibiotics in these concentrations cause a redshift in wavelength due to the dipole coupling among the plasmons of the neighboring aggregated GNPs. As a result, the intensity of absorption decreases, and the peak shifts toward higher wavelengths. Also, these results showed that antibiotic binding to an antibody increases the absorption of the wavelength of a maximum, which shows that the antibody is sensitive to 1 nM of β-lactam antibiotics (ampicillin, penicillin G, amoxicillin, carbenicillin, and oxacillin). Because of the minimal amount of antibiotics added (1 nM), the intensity of absorption and the wavelength of a maximum changed. Meanwhile, the results indicated that wavelength of a maximum (λ_{LSPR}) increased with increasing concentration of β-lactam antibiotics from 1 nM to 1 μM (ampicillin), 1 nM to 0.1 μM (penicillin G), 1 nM to 1 μM (amoxicillin), 1 nM to 0.1 μM (carbenicillin), and 1 nM to 0.01 nM (oxacillin). With excessive increase in antibiotics concentration (1μM to 0.1 mM ampicillin, 0.1 μM to 0.1 mM penicillin G, 1 μM to 1 mM amoxicillin, 0.1 μM to 0.1 mM carbenicillin, and 0.01 nM to 1 mM oxacillin), the wavelength of a maximum does not change, which demonstrates the saturation state in the detection of antibiotics (Fig. 8). The reason is that in high concentrations of the target molecule in the environment, the amount of accumulation will increase. In extremely high concentrations, it will become a vast aggregation. In other words, to increase the concentration of the antibiotic molecule in the environment,

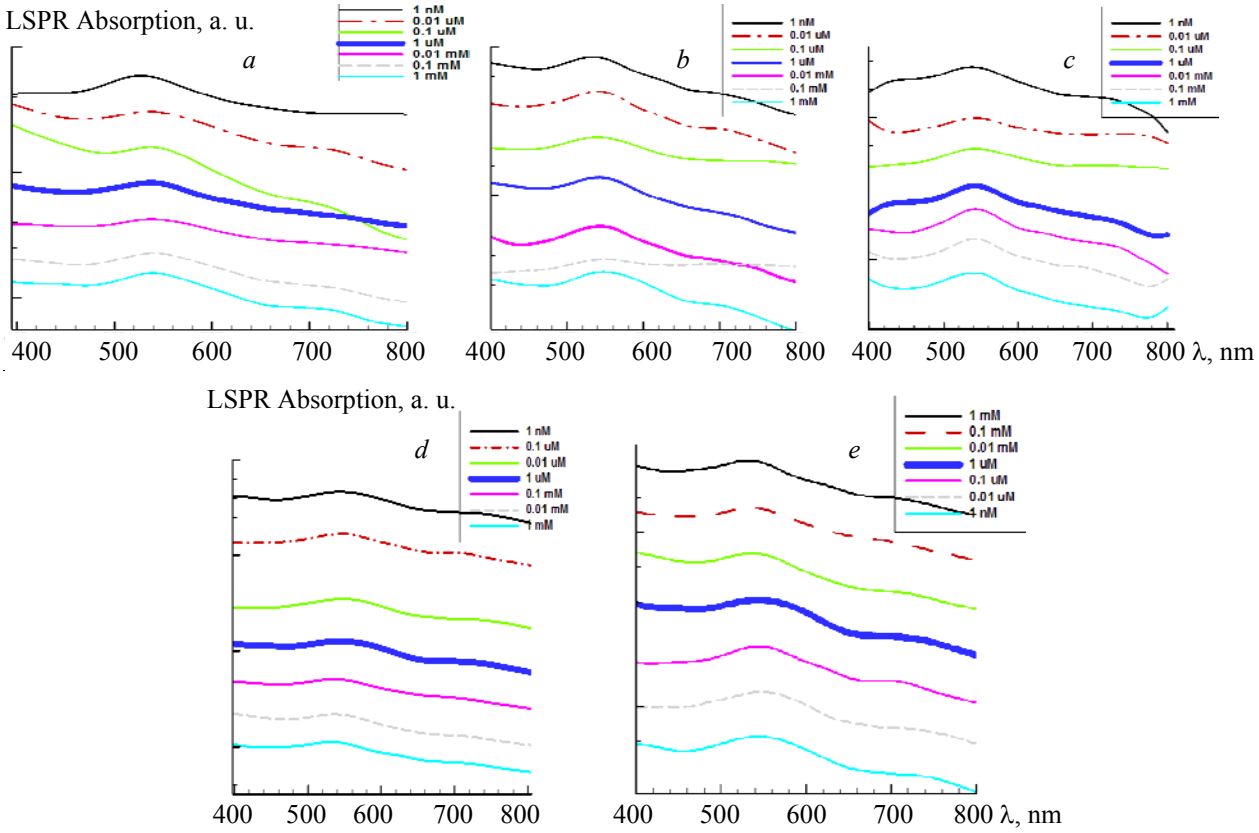

Fig. 7. LSPR absorption spectra changes of a GNPs solution upon the addition of β-lactam antibiotics in the concentration range of 1 nM to 1 mM (a – ampicillin, b – penicillin G, c – amoxicillin, d – carbenicillin, and e – oxacillin).

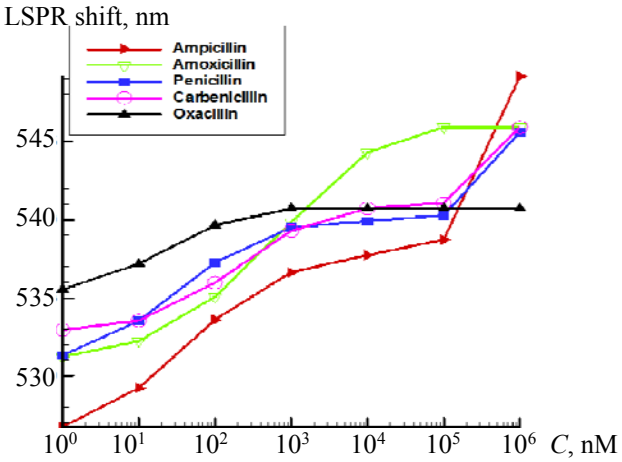

Fig. 8. LSPR shift absorption spectra changes of a GNPs solution upon the addition of β-lactam antibiotics (ampicillin, penicillin G, amoxicillin, carbenicillin, and oxacillin) in the concentration range of 1 nM to 1 mM.

the amount of antibody bound to the target molecule will be greater. Consequently, the active site of antibody is filled and there is no empty capacity to detect antibiotic. In this state, the graph becomes saturated and horizontal (Fig. 8). Change of wavelength peak for ampicillin, penicillin G, and carbenicillin is similar (Fig. 8). This indicates that the antibody has a similar behavior in the detection of these antibiotics. The wavelength of a maximum in the amoxicillin curve was compared to other β-lactam antibiotics at higher saturated concentrations. Therefore, it can be concluded that this antibody is more specific for the detection of amoxicillin and has higher detectability. (Fig. 8). As seen in Fig. 8, oxacillin was saturated very soon and had a horizontal mode, which indicates that the antibody has a very low detection capability for oxacillin. To explain, the structure of the active site of the antibody is more similar to the structure of amoxicillin and, on the other hand, the structure of the active site is less similar to the structure of oxacillin. Wang et al. [37] showed that the wavelength of a maximum migrates significantly with increase in the concentration of kanamycin in the range of 10 nM to 1 μM.

Conclusions. Gold nanoparticles (GNPs)-based colorimetric sensors have attracted great attention due to the excellent properties for the detection of residual drugs in food. In this study, GNPs conjugated with antibody were used for the colorimetric detection of β-lactam antibiotics (such as ampicillin, amoxicillin, penicillin G, oxacillin and carbenicillin). Structural analysis by XRD showed that nanoparticles have a crystalline structure with Miller indexes (1 1 1), (2 0 0), (2 2 0), and (3 1 1) in the cubic network. FTIR spectroscopy analysis revealed that the high stability of GNPs could be attributed to the extract used as a reducing agent in the production of GNPs. A pH of 8 and a concentration of 8.4 μg of antibody at 1 mL GNPs solution were selected as the best pH and concentration of antibody for conjugation. The LSPR wavelength of GNPs increased with higher concentration of β-lactam antibiotics. With rising concentration of ampicillin, penicillin G, and carbenicillin, the wavelength of a maximum changed, and after saturation of antibiotics concentration, the curve reached a plateau. However, regarding amoxicillin, the saturation concentration is much higher, indicating that the antibody is more specific for the detection of amoxicillin. In contrast, the system has a very low detection capability for this oxacillin. Also, the results showed that the antibody is sensitive to 1 nM of the five β-lactam antibiotics studied.

Conflict of interest. The author(s) declared no potential conflicts of interest concerning the research, authorship, and/or publication of this article.

Acknowledgments. This article is a part of a Ph.D. thesis approved at the University of Tabriz. This work was financially supported by Iran Nanotechnology Initiative Council (Grant code: 136472). The authors would like to thank Prof. Mohammad Javad Rasaee from Tarbiat Modares University, Dr. Seyed Mohammad Amini from Iran University of Medical Sciences, and Mr. Gholamreza Behrouzi, Mr. Babak Farshid, Miss Zahra Abolghasemi-Fakhri, and Mrs. Samira Tizchang for their very useful comments. We thank Rojan Azma Co. and its personnel for supporting research equipment. Finally, we thank Daneshmand Research & Development Institute and Mostazafan Foundation of Islamic Revolution.

REFERENCES

1. V. Tamošiūnas, A. Padarauskas, *Chromatographia*, **67**, 783–788 (2008), https://doi.org/10.1365/s10337-008-0579-5.
2. T. Śniegocki, A. Posyniak, J. Żmudzki, *Bull. Vet. Inst. Pulawy*, **51**, 59–64 (2007).
3. W. B. Shim, J. S. Kim, M. G. Kim, D. H. Chung, *J. Food Sci.*, **78**, 1575–1581 (2013).
4. N. V. Gasilova, S. A. Eremin, *J. Anal. Chem*., **65**, 255–259 (2010), https://doi.org/10.1134/s1061934810030081.
5. F. Conzuelo, M. Gamella, S. Campuzano, D. G. Pinacho, A. J. Reviejo, M. P. Marco, J. M. Pingarrón, *Biosens. Bioelectron*., **36**, 81–88 (2012), https://doi.org/10.1016/j.bios.2012.03.044.
6. E. Kazemi, S. Dadfarnia, A. Mohammad, H. Shabani, M. R. Fattahi, J. Khodaveisi, *Spectrochim. Acta A : Mol. Biomol. Spectrosc.*, **187**, 30–35 (2017), https://doi.org/10.1016/j.saa.2017.06.023.
7. N. Bi, M. Hu, H. Zhu, H. Qi, Y. Tian, H. Zhang, *Spectrochim. Acta A: Mol. Biomol. Spectrosc*., **107**, 24–30 (2013), https://doi.org/10.1016/j.saa.2013.01.014.
8. P. Cyganowski, D. Jermakowicz-Bartkowiak, P. Jamroz, P. Pohl, A. Dzimitrowicz, *Colloids Surf. A*, **582**, 123886 (2019), https://doi.org/10.1016/j.colsurfa.2019.123886.
9. K. Hamaguchi, H. Kawasaki, R. Arakawa, *Colloids Surf. A, Physicochem. Eng. Asp.*, **367**, 167–173 (2010), https://doi.org/10.1016/j.colsurfa.2010.07.006.
10. Y. Huang, K. Ma, K. Kang, M. Zhao, Z. Zhang, Y. Liu, *Colloids Surf. A, Physicochem. Eng. Asp*., **421**, 101–108 (2013), https://doi.org/10.1016/j.colsurfa.2012.12.050.
11. X. Li, L. Jiang, Q. Zhan, J. Qian, S. He, *Colloids Surf. A, Physicochem. Eng. Asp*., **332**, 172–179 (2009), https://doi.org/10.1016/j.colsurfa.2008.09.009.
12. S. Golmohammadi, M. Etemadi, *J. Appl. Spectrosc*., **86**, 925 (2019), https://doi.org/10.1007/s10812-019-00917-y.
13. C. Karami, A. Alizadeh, M. A. Taher, Z. Hamidi, B. Bahrami, *J. Appl. Spectrosc*., **83**, 687–693 (2016), https://doi.org/10.1007/s10812-016-0349-3
14. G. P. Sahoo, H. Bar, D. K. Bhui, P. Sarkar, S. Samanta, S. Pyne, S. Ash, A. Misra, *Colloids Surf. A*, *Physicochem. Eng. Asp*., **375**, 30–34 (2011), https://doi.org/10.1016/j.colsurfa.2010.11.033.
15. M. Singh, I. Sinha, A. K. Singh, R. K. Mandal, *Colloids Surf. A, Physicochem. Eng. Asp*., **384**, 668–674 (2011), https://doi.org/10.1016/j.colsurfa.2011.05.037.
16. P. Vaccarello, L. Tran, J. Meinen, C. Kwon, Y. Abate, Y. Shon, *Colloids Surf. A*, *Physicochem. Eng. Asp.*, **402**, 146–151 (2012), https://doi.org/10.1016/j.colsurfa.2012.03.041.
17. Y. Yang, Q. Cui, Q. Cao, L. Li, *Colloids Surf. A, Physicochem. Eng. Asp*., **503**, 28–33 (2016), https://doi.org/10.1016/j.colsurfa.2016.05.026.
18. J. Ye, K. Bonroy, F. Frederix, J. D. Haen, G. Maes, G. Borghs, *Colloids Surf. A*, *Physicochem. Eng. Asp*., **321**, 313–317 (2008), https://doi.org/10.1016/j.colsurfa.2008.01.028.
19. K. S. McKeating, M. Couture, M. P. Dinel, S. Garneau-Tsodikova, J. F. Masson, *Analyst*., **141**, 5120–5126 (2016), https://doi.org/10.1039/c6an00540c.
20. L. Chen, Z. Wang, M. Ferreri, J. Su, B. Han, *J. Agric. Food Chem*., **57**, 4674–4679 (2009), https://doi.org/10.1021/jf900433d.
21. A. Singh, M. Sharma, A. Batra, *J. Optoelectron. Biomed. Mater*., **5**, 27–32 (2013).
22. C. George, I. Sergiel, A. Dzimitrowicz, P. Jamro, T. Kozlecki, P. Pohl, *Preparation and characterization of gold nanoparticles prepared with aqueous extracts of Lamiaceae plants and the effect of follow-up treatment with atmospheric pressure glow microdischarge* (2016), https://doi.org/10.1016/j.arabjc.2016.04.004.
23. J. Huang, Q. Li, D. Sun, Y. Lu, Y. Su, X. Yang, H. Wang, Y. Wang, W. Shao, N. He, J. Hong, C. Chen, *Nanotechnology*, **80**, 285–290 (2007), https://doi.org/10.1088/0957-4484/18/10/105104.
24. J. M. B. Res, G. Oza, S. Pandey, A. Gupta, R. Kesarkar, M. Sharon, W. Ambernath, *J. Microbiol. Biotechnol*., **2**, 511–515 (2012).
25. C. Zhou, X. Zhang, X. Huang, X. Guo, Q. Cai, S. Zhu, *Sensors* (*Switzerland*), **14**, 21872–21888 (2014), https://doi.org/10.3390/s141121872.
26. A. Aljabali, Y. Akkam, M. Al Zoubi, K. Al-Batayneh, B. Al-Trad, O. Abo Alrob, A. Alkilany, M. Benamara, D. Evans, *Nanomaterials*, **8**, 1–15 (2018). https://doi.org/10.3390/nano8030174.
27. H. Mohammadi, M. Hafezi, S. Hesaraki, M. M. Sepantafar, *Nanomed. J*., **2**, 217–222 (2015), https://doi.org/10.7508/nmj.

28. N. T. Ndeh, S. Maensiri, D. Maensiri, *Adv. Nat. Sci. Nanosci. Nanotechnol.*, **8**, aa724a (2017), https://doi.org/10.1088/2043-6254/aa724a.
29. S. Goldmeier, K. De Angelis, K. R. Casali, C. Vilodre, F. Consolim-Colombo, A. B. Klein, R. Plentz, P. Spritzer, M. C. Irigoyen, *Am. J. Transl. Res*., **6**, 91–101 (2014), https://doi.org/10.1016/j.saa.2011.02.051.
30. S. A. Aromal, V. K. Vidhu, D. Philip, *Spectrochim. Acta A: Mol. Biomol. Spectrosc*., **85**, 99–104 (2012), https://doi.org/10.1016/j.saa.2011.09.035.
31. G. M. Corp, C. Astro, G. M. C. Safari, *Environ. Sci. Technol*., **37**, 3458–3466 (2003).
32. H. Borchert, E. V. Shevchenko, A. Robert, I. Mekis, A. Kornowski, G. Grübel, H. Weller, *Langmuir*, **21**, 1931–1936 (2005), https://doi.org/10.1021/la0477183.
33. D. K. Singh, R. Jagannathan, P. Khandelwal, P. M. Abraham, P. Poddar, *Nanoscale*, **5**, 1882–1893 (2013), https://doi.org/10.1039/c2nr33776b.
34. C. N. R. Rao, A. K. Cheetham, *J. Mater. Chem*., **11**, 2887–2894 (2001), https://doi.org/10.1039/b105058n.
35. L. Liu, Y. Chen, S. Song, Q. Zheng, X. Wu, H. Kuang, *Food Agric. Immunol*., **28**, 1283–1292 (2017), https://doi.org/10.1080/09540105.2017.1337084.
36. H. Zhang, W. Li, Z. Sheng, H. Han, Q. He, *Analyst*, **135**, 1680–1685 (2010), https://doi.org/10.1039/c0an00025f.
37. Ch. Wang, J. Liu, X. Han, Ch. Liu, Y. Tian, N. Lhou, *Analyt. Method*s (**2017**), https://doi.org/10.1039/C7AY01685A.